

---

# UCSF-PDGM-VQA: Visual Question Answering dataset for brain tumor MRI interpretation

---

**Shiv Ghosh\***

Fung Institute for Engineering Leadership  
University of California, Berkeley  
Berkeley, CA 94709  
shiv.ghosh@berkeley.edu

**Junayd Lateef\***

Fung Institute for Engineering Leadership  
University of California, Berkeley  
Berkeley, CA 94709  
jlateef@berkeley.edu

**Chih-Hua Liu\***

Fung Institute for Engineering Leadership  
University of California, Berkeley  
Berkeley, CA 94709  
ch.liu@berkeley.edu

**Yannan Yu**

Department of Radiology  
University of California, San Francisco  
San Francisco, CA 94158  
yannan.yu@ucsf.edu

**Andreas M. Rauschecker**

Department of Radiology  
University of California, San Francisco  
San Francisco, CA 94143  
andreas.rauschecker@ucsf.edu

**Madhumita Sushil**

Division of Clinical Informatics and Digital Transformation and Department of Neurological Surgery  
University of California, San Francisco  
San Francisco, CA 94158  
Madhumita.Sushil@ucsf.edu

## Abstract

Brain tumor diagnosis is largely dependent on Magnetic Resonance Imaging (MRI) evaluation, which requires radiologists to synthesize thousands of images across multiple 3D sequences and longitudinal studies. This process requires advanced neuro-radiology training, poses substantial cognitive load, and is highly time-consuming. Despite increasing demands in radiology, this expertise is difficult to scale, straining the current health systems. Vision-Language Models (VLMs) provide an opportunity to reduce this burden through a semi-automated, interactive interpretation of complex brain MRIs. However, they are currently underutilized in neuro-oncology due to a lack of specialized benchmarks for evaluating them. We introduce a clinically relevant visual question answering (VQA) benchmark — the UCSF-PDGM-VQA dataset — consisting of 2,387 QA pairs from 473 glioma-related MRI studies in the public UCSF-PDGM dataset. We further establish a performance baseline for six state-of-the-art vision-language models (VLMs) and one large language model on this dataset. We find that current models are incapable of effectively processing multi-sequence, 3-dimensional MRI scans, thus resulting in a suppression of visual features and over-reliance on language priors, causing modality collapse. These findings underscore a critical deficiency in current model reliability and safety within clinical settings, necessitating the development of robust, domain-specific VLMs.

# 1 Introduction

Primary brain and central nervous system (CNS) tumors impact more than 1 million individuals in the United States with an incidence of nearly 500,000 cases a year [Price et al., 2024]. Brain tumors are a leading cause of death, with the median survival for an aggressive subtype called glioblastoma being only 12–18 months. Timely diagnosis and quick action are thus critical. Magnetic resonance imaging (MRI) is the primary imaging modality for detecting and monitoring brain tumors. However, interpreting brain tumor MRI scans is complex and time-consuming, as radiologists must analyze thousands of image slices, integrate information from multiple imaging sequences, and compare findings at multiple timepoints. On average, it takes 11–18 minutes to read a single brain MRI scan [Al Yassin et al., 2018], with more complex scans requiring hours. Prolonged periods of clinical image interpretation have been associated with a decrease in abnormality detection performance among radiologists Krupinski et al. [2010].

Recent advances in vision-language models (VLMs) are promising for developing an interactive radiology copilot to enable easier interpretation of complex scans. Despite the recent popularity of VLMs, as well as VQA with VLMs, their applications and use for complex diseases like brain tumors have been limited. Existing datasets for VQA are either limited to anatomies other than brain, or are artificially simplified, providing only 2-dimensional (2D) images when real-world studies instead require the processing of multiple 3-dimensional (3D) series. Clinical brain MRI studies routinely collect scans of types T1 pre-contrast, T1 post-contrast, T2, FLAIR, diffusion, SWI, and perfusion for accurate interpretation. Each scan type reveals a different aspect of the brain tumor by imaging distinct variations in tissue signal intensity to better view the brain tumor-associated abnormality. For example, T1 scans without contrast are used to understand the baseline anatomical view of the brain, T1 post-contrast scans provide information related to where the blood-brain barrier is disrupted or the tumor’s vascularity is abnormal, and T2 FLAIR scans are useful for identifying edema and the boundaries of the tumor [Villanueva-Meyer et al., 2017]. A joint analysis of all these scan types is critical to ensure an accurate interpretation. Furthermore, new scans are often compared to prior scans to understand longitudinal changes associated with either disease progression or treatment response, which is critical to determine the next steps for the patient [Villanueva-Meyer et al., 2017]. The simplifications within existing datasets limit clinically significant progress, thus constraining the translation of VLMs or VQA into real-world clinical workflows.

To bridge this gap, we introduce a VQA dataset comprising clinically relevant concepts and scans, the UCSF-PDGM-VQA dataset, which provides a set of 2,387 closed-ended question-answer pairs answerable from 473 brain MRI studies for patients with diffuse gliomas. Each MRI study includes all imaging series collected during routine patient care, including the sequences described earlier. While the dataset includes scans only at a single time point — preoperative scans, it is the first step towards developing a VQA dataset that reflects the complexity of real-world brain MRI processing.

We further evaluated popular open-weight, clinical VLMs on this dataset to assess model performance. We identified key challenges in integrating all imaging series and thousands of slices in existing models - they are simply incapable of processing data of this complexity, resolution, and scale. Downsampling vision input to a few slices supported by existing models, we identified significant performance gaps; the best performing model, the MedGemma-1.5 model [Sellergren et al., 2025], scored only 63.57% accuracy on the task, with other models being significantly worse. Our ablation studies revealed a clear instance of modality collapse, wherein the multimodal models relied strictly on textual cues rather than visual data. This is evidenced by several VLMs improving when the imaging slice was replaced with a blank input. Notably, Lingshu-32B [Team et al., 2025b] achieved the highest overall accuracy observed (66.04%) when provided only with a blank image. This finding is further reinforced by the text-only LLM Qwen3-8B matching the performance of the multimodal MedGemma model. Alongside this modality collapse, the models exhibited a strong positional language bias: scores changed significantly when answer options were reordered despite identical inputs, confirming a reliance on structural heuristics rather than actual clinical reasoning. This highlights a key safety concern related to the use of VLMs in clinical settings: model responses are biased towards text prompts rather than the actual image demonstrating the disease presentation. This is deeply concerning, especially when, during a clinical review, the questions were deemed to be unanswerable without the accompanying radiology image. Together, these findings highlight the need for developing VLMs that are not only capable of processing multi-series 3D imaging, but also those that are robust to modality collapse to ensure that they can be safely translated for real-world clinical use.

To summarize, our key contributions are as follows:

- We curated the first multiple-choice VQA dataset for brain tumor-associated MRI interpretation. The dataset will be made available on PhysioNet to enable future analysis on newer VLMs.
- We benchmarked the capabilities of existing VLMs on this dataset, comparing model performance with clinical performance and identifying key performance gaps. All accompanying source code has been made available on Github <sup>1</sup>.
- We evaluated vulnerabilities of existing VLMs on this VQA task, demonstrating the lack of effective integration of the vision modality, thus highlighting the risks associated with the clinical deployment of these models.
- We designed a prototype graphical user interface enabling intuitive visualization and interaction with the underlying datasets and integrated models, hosted publicly at **redacted**.

## 2 Related Work

### 2.1 Existing Biomedical VQA Datasets

Several biomedical vision-language datasets are available publicly, enabling research on tasks such as biomedical VQA. Some notable VQA datasets include RadVisDial Kovaleva et al. [2019], Path-VQA He et al. [2020], VQA-Med (2021) Ben Abacha et al. [2021], MIMIC CXR VQA Bae et al. [2023], Medical-Diff-VQA Hu et al. [2025], VQA-RAD[Lau et al., 2018], SLAKE[Liu et al., 2021], OVQA [Huang et al., 2022], M3D-VQA Bai et al. [2024], and PMC-VQA Zhang et al. [2023b] (Table 1), and additional vision-language datasets like CT-RATE [Hamamci et al., 2026] that do not provide a VQA subset. The brain is often not included as an anatomical structure in these datasets. Furthermore, many existing datasets are curated by retrieving images from public medical resources and repurposing image captions into question-answer pairs. Thus, 3D data, such as computed tomography (CT) and magnetic resonance imaging (MRI) exams, end up being represented as 2D, resulting in significant information loss and limiting their clinical utility. In contrast, real-world CT and MRI scans comprise thousands of 2D slices that together form a single 3D imaging series. Moreover, multiple series, such as pre-contrast and contrast-enhanced, and more advanced MRI-specific sequences, such as T2, FLAIR, and DWI, are jointly processed for reliable inference at a single time point. To our knowledge, the UCSF-PDGM-VQA dataset developed in this study is the first publicly available VQA dataset to encompass multiple brain anatomy imaging sequences, enabling VQA tasks in a more clinically aligned setting. Finally, questions included within existing datasets span topics such as imaging techniques, anatomical location, and organ systems visible, which are trivial for radiologists and not clinically meaningful for interpreting the scan [Mishra et al., 2025]. In this study, we focus on VQA pairs derived from the findings and interpretations of the underlying radiology exam, creating a more clinically relevant dataset.

Table 1: Comparison between existing and proposed clinical VQA datasets

| Dataset           | Modalities            | Anatomy                                     | 2D or 3D | Multi-series? | Size    | QA format           | Curation       |
|-------------------|-----------------------|---|----------|---------------|---------|---------------------|----------------|
| RadVisDial (2019) | X-ray                 | Chest                                       | 2D       | No            | 455,300 | Closed-ended        | Automated      |
| Path-VQA          | Pathology             | Body Tissues                                | 2D       | No            | 32,799  | Open-, Closed-ended | Semi-automated |
| VQA-Med (2021)    | X-ray, CT, MRI        | Breast, Skull, Face, Spine, Musculoskeletal | 2D       | No            | 5,000   | Open-ended          | Semi-automated |
| MIMIC CXR VQA     | X-ray                 | Chest                                       | 2D       | No            | 377,391 | Open-, Closed-ended | Automated      |
| Medical-Diff-VQA  | X-ray                 | Chest                                       | 2D       | No            | 700,703 | Open-ended          | Semi-automated |
| VQA-RAD           | X-ray, CT, MRI        | Head, Chest, Abdomen                        | 2D       | Yes           | 3,515   | Open-, Closed-ended | Semi-automated |
| SLAKE             | X-ray, CT, MRI        | Head, Chest, Abdomen                        | 2D       | No            | 14,000  | Open-, Closed-ended | Manual         |
| OVQA              | X-ray, CT             | Head, Chest, Leg, Hand                      | 2D       | No            | 19,020  | Open-, Closed-ended | Semi-automated |
| M3D-VQA           | CT                    | Mainly Liver, Spleen, Kidney, Lung          | 3D       | No            | 509,755 | Closed-ended        | Semi-automated |
| PMC-VQA           | Mainly X-ray, CT, MRI | Brain, Lung, Heart, Liver                   | 2D       | No            | 226,946 | Closed-ended        | Semi-automated |
| UCSF-PDGM-VQA     | MRI                   | Brain                                       | 3D       | Yes           | 2,387   | Closed-ended        | Semi-automated |

### 2.2 Existing clinical vision-language models

Several multimodal models, such as MedFlamingo Moor et al. [2023], LLaVA-Med Li et al. [2023], BiomedCLIP Zhang et al. [2025], PubMedCLIP Eslami et al. [2023], MPMA Zhang et al. [2023a], VILA-M3 Nath et al. [2025], Med3DVLM Xin et al. [2025], MedGemma-1.5 Sellergren et al. [2025], Lingshu Team et al. [2025b], Merlin Blankemeier et al. [2026], CT-CLIP Hamamci et al.

<sup>1</sup><https://github.com/m2ai-lab/VLM-Brain-Tumor-QA-pipeline>

[2026], Pillar-0 Agrawal et al. [2025b], CALM-VLM Dhinagar et al. [2026], and Prima Lyu et al. [2026], have been recently developed for medical image analysis (Table 2). These models typically build upon pretrained medical imaging and medical language backbones, which are subsequently refined and fine-tuned for specific imaging modalities or downstream tasks. Fusion strategies range from contrastive learning–based modality alignment to cross-modal attention and instruction tuning. However, despite continued domain-specific training, existing architectures remain limited in their ability to fully capture clinically relevant information. In most approaches, 3D medical images are resampled and standardized to a fixed tensor size, effectively reducing the volume to a predetermined number of slices before inference. While this standardization enables efficient model training, it can limit the volumetric context present in the original scan. Recent models such as Pillar-0 [Agrawal et al., 2025b] and Prima [Lyu et al., 2026] attempt to address this limitation by processing complete 3D volumes; however, these approaches remain both anatomy- and modality-specific and are not yet trained for zero-shot VQA. Table 2 provides a list of available clinical VLMs, and their key limitations for VQA over brain MRI data.

Table 2: Existing clinical vision-language models and their key limitations for brain MRI VQA.

| Model           | Vision Encoder                   | Text Encoder                            | Fusion Strategy   | Key Limitation                                     |
|-----------------|----------------------------------|---|---|--|
| MedFlamingo     | CLIP ViT/L-14                    | LLaMA-7B Touvron et al. [2023]          | Gated Cross-Attention                                   | Lacks neuro-oncology data, no VQA                  |
| LLaVA-Med       | CLIP ViT (2D)                    | Vicuna Chiang et al. [2023]             | Linear Projection                                       | 2D image input instead of 3D                       |
| BiomedCLIP      | CLIP ViT-B/16                    | GPT-2 Radford et al. [2019]             | Cosine Similarity of Modality pairs                     | 2D image input instead of 3D                       |
| PubMedCLIP      | CLIP-ViT/B-32                    | OpenAI CLIP Radford et al. [2021]       | Scaled pair-wise Cosine Similarity                      | 2D image input instead of 3D                       |
| MPMA            | CLIP-ViT/B                       | CXR-Bert Boecking et al. [2022]         | Global and Local Alignment                              | Lack of MRI VQA training                           |
| VILA-M3         | OpenAI’s CLIP-L                  | Vicuna Chiang et al. [2023]             | Auxiliary Token Injection                               | High inference latency from multiple expert models |
| Med3DMLM        | DCFormer (3D) Ates et al. [2025] | ClinicalBERT Wang et al. [2023]         | MLP-Mixer Projector                                     | Lacks neuro-oncology data                          |
| MedGemma-1.5    | MedSigLIP                        | Gemma 3 [Team et al., 2025a]            | Voxel Mapping   | Lacks neuro-oncology data                          |
| MedImageInsight | DaViT-360M Ding et al. [2022]    | Florence-252M Yuan et al. [2021]        | Unified Contrastive Learning (UniCL) Yang et al. [2022] | 2D MRI slice input instead of 3D                   |
| Lingshu         | Qwen2.5-VL Bai et al. [2025]     | Qwen2.5-VL Bai et al. [2025]            | MLP-based Projector                                     | 2D MRI slice input instead of 3D                   |
| Merlin          | ED ResNet152                     | Clinical Longformer Li et al. [2022]    | Cross-modal retrieval with ICD codes                    | Only CT support, no MRI training                   |
| CT-CLIP         | CLIP                             | CXR-Bert Boecking et al. [2022]         | Contrastive Loss  | Only CT support, no MRI training                   |
| Pillar-0        | Atlas Agrawal et al. [2025a]     | Qwen3 Yang et al. [2025]                | Asymmetric contrastive pretraining                      | Lacks neuro-oncology data                          |
| CALM-VLM        | DCFormer (3D) Ates et al. [2025] | Qwen-2.5-7B-Instruct Qwen et al. [2025] | MLP-mixer architecture                                  | For Alzheimer’s classification; not VQA            |
| Prima           | CLIP-ViT                         | GPT-2 Radford et al. [2019]             | Cosine Similarity                                       | Not trained for VQA                                |

### 3 Methods

We aim to address the limitations of existing clinical VQA datasets in the context of brain MRI interpretation. Specifically, we aim to curate a dataset that combines multi-series, multi-slice 3D brain MRIs with clinically-relevant questions to enable the benchmarking of existing and new VLMs on VQA tasks for neuro-oncology. The study was conducted under an approved institutional IRB.

#### 3.1 UCSF-PDGM brain MRI dataset

University of California, San Francisco Preoperative Diffuse Glioma MRI (UCSF-PDGM) dataset [Calabrese et al., 2022b,a] consists of pre-operative brain MRIs for 501 patients with diffuse gliomas. The MRI studies were conducted using a standardized 3-T protocol that predominantly employed three-dimensional (3D) imaging, including diffusion and perfusion imaging for more advanced clinical interpretation. The imaging dataset is available publicly upon signing a data use agreement.

#### 3.2 QA pair generation

We used the same set of brain MRI scans as those included in the UCSF-PDGM study, along with their corresponding radiology reports documenting the study’s key findings and radiologic impressions, which were repurposed into multiple-choice question-answer (QA) pairs. 19 of 501 studies were excluded due to data mapping challenges. The pipeline comprised two phases:

1. Generation: A large-language model (LLM), specifically the GPT-4o model [OpenAI et al., 2024], was prompted to generate up to 20 question-answer pairs per study, with four options per question, based on the *Findings* and *Impression* sections of the report. The model was constrained to generate only questions whose correct answers were contained within these sections and to avoid including any unanswerable questions, such as those related to imaging technique, clinical history, disease progression, or a different anatomy, like the spine. The model was instructed to exclude options such as *Not Discussed* or *None of the above*, retaining only those questions that could be answered based on the imaging data. Finally, we opted for a closed-ended, multiple-choice QA setting to enable robust, automated evaluation of model capabilities. Although an open-ended QA format may be more desirable in real-world settings, it is challenging to scale clinical evaluations across multiple models,

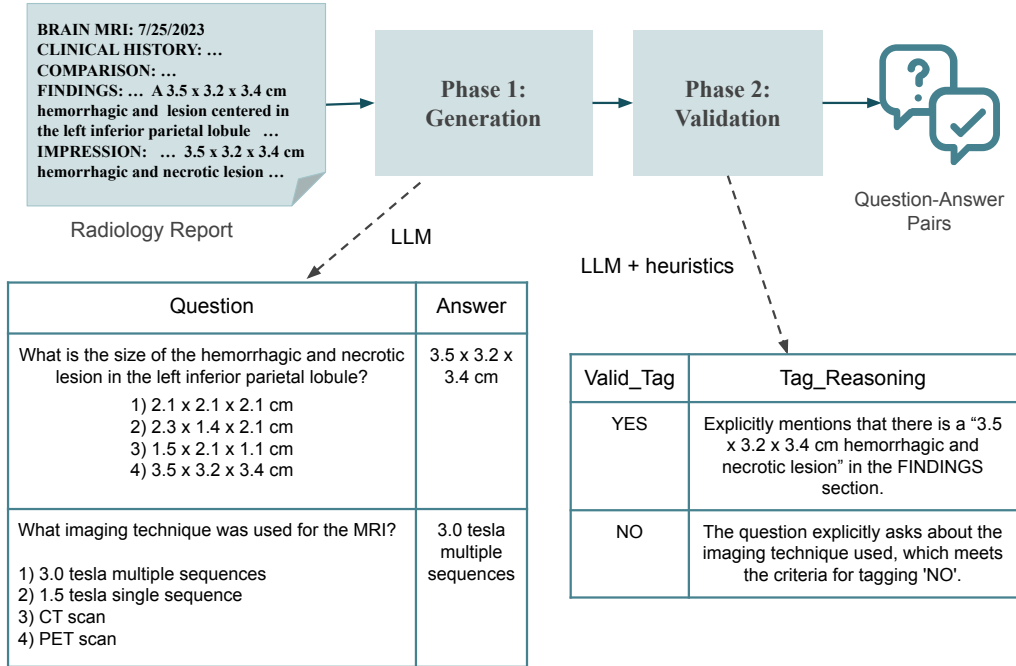


Figure 1: Figure showing the data generation pipeline, along with the intermediate output in each phase. The generation phase produces candidate question-answer pairs, while the validation phase filters irrelevant or unanswerable QA pairs.

runs, and ablation settings, thus providing an incomplete view of model performance and robustness. While LLM-as-a-judge methods are popular, there are well-known limitations of these methods for model evaluation Zheng et al. [2023], particularly for domains requiring advanced knowledge, such as neuro-radiology.

2. **Validation and Filtering:** A separate instance of the GPT-5.2 model [OpenAI, 2025] was prompted to use normal reasoning effort to determine whether: (a) the generated question-answer pairs were answerable solely from the image and the report, (b) to reduce ambiguity, ensure that the laterality or location of a concerned mass or lesion within the brain was specified within the question, (c) to ensure that the questions about lesion size included the spatial directions along which the size should be reported, and (d) to rephrase any unanswerable or concerning questions. A keyword-based filter was subsequently applied to remove any question-answer pairs that contained keywords indicating unanswerable questions, such as those requiring either clinical history, temporal information, or external data to be answered correctly (e.g., postsurgical, metastasis, recurrent, spine). Duplicate questions were additionally removed through a lexical match. Manual quality validation was performed on a set of 200 QA pairs iteratively before generating the final dataset. A final subset of 75 questions was evaluated by a neuro-radiology fellow for clinical relevance and answerability.

The full pipeline is illustrated in Figure 1, the specific model settings and prompt for the generation phase are placed in Appendix A, the generation phase JSON output structure is in Appendix B, the specific model settings and prompt for the validation phase are placed in Appendix C, and the validation phase JSON output structure is in Appendix D.

### 3.3 Modeling Baselines

We evaluated the following vision-language models on the UCSF-PDGM-VQA dataset to establish performance benchmarks in a zero-shot setting: LLaVa-Med [Li et al., 2023], MedImageInsight [Codella et al., 2024], Med3DVLM [Xin et al., 2025], Lingshu [Team et al., 2025b], MedGemma 1.5 [Sellergren et al., 2025], and the closed-weight GPT5-mini model [Singh et al., 2026]. Since these

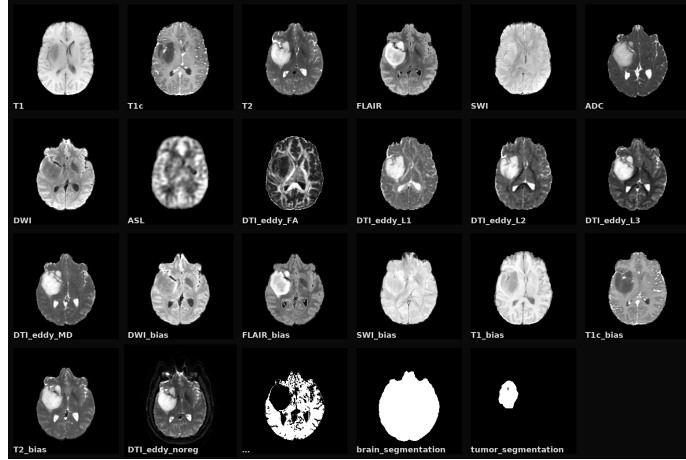


Figure 2: Example of Axial MRI montage

models cannot process an entire MRI study at once, and several models also do not support multi-slice input, initial experiments evaluated different input representations for robust model performance. The most informative slices were selected as those containing the highest tumor volume, identified using a brain tumor segmentation model, the Swin-UNETR model [Hatamizadeh et al., 2021], which was previously trained on the BRaTS dataset for brain tumor segmentation [Baid et al., 2021]. For models only capable of supporting a single image, axial orientation of the FLAIR scans were prioritized. Additionally, a second setting was tested, which combined the highest tumor volume slices from all axial imaging series, along with brain and tumor segmentations, into a single composite grid to provide maximal information through a single image input (Composite Montage, example in Figure 2). This enabled us to provide all key imaging slices as input models constrained to process a single scan input.

Only two models — the MedGemma-1.5 model and GPT5-mini model — were capable of supporting multiple image inputs, and thus they were evaluated in an additional multi-slice input configuration. Under this setting, all axial slices corresponding to the highest tumor volume, across all imaging series, were input as separate images to provide responses to the QA pair. The slices selected corresponded to the Composite Montage setting, but instead of providing them as a montage input, they were provided to the model as separate images. This created an input of up to 23 image slices per MRI study, mapped to each QA pair. We further tested a multiple montage input to these models as well, which provided as input montage composite images in the axial, sagittal, and coronal orientations.

Since the UCSF-PDGM-VQA dataset is a closed-ended, multiple-choice QA dataset, model accuracy was reported as the performance metric. To establish a reliable performance bound, zero-shot inference was conducted three times, with results averaged across all runs.

### 3.4 Clinical performance

To ensure the clinical relevance of the generated dataset and to validate the LLMs’s ability to produce high-quality VQA pairs, we conducted a human evaluation on a random subsample of 75 questions. These questions were provided to a neuroradiology fellow to establish an upper-bound clinical baseline to evaluate VLM architectures. Human evaluation interface consisted of four components: (1) human expert agreement on the correct answers, (2) clinical relevance of the question-answer pair, (3) the clinician’s self-reported confidence score for their answer, and (4) an assessment of whether the question could be accurately answered using the provided image. This allows for quantifying the quality of the dataset, while also contextualizing VLM performance against radiology performance, providing a baseline to evaluate future model architectures.

### 3.5 Robustness tests / Ablation analysis

To evaluate potential modality collapse and the impact of language priors, we conducted multiple ablation studies with the following settings:

**Text-only LLM baseline:** We used the Qwen3-8B LLM [Yang et al., 2025] to establish a text-only baseline, comparing VLM performance against a language-only model. We opted for the Qwen model, specifically given its strong performance on diverse tasks.

**Blank image input to VLMs:** All MRI scans were replaced with a plain black ("blank") image to evaluate the ability of VLMs to ground their responses on image input.

**Shuffled choice options:** We randomized the order of the multiple-choice options to ensure that answer selection was driven by actual understanding rather than statistical positional bias.

## 4 Results

### 4.1 Dataset Statistics and Composition

The UCSF-PDGM-VQA dataset curated in this study includes 2,387 question-answer pairs, with four multiple-choice options each, corresponding to 473 brain MRI studies. Key dataset statistics are presented in Table 3. The QA pairs span questions related to tumor size, location, anatomical changes, and tumor diagnosis. Sample QA pairs are provided in the Appendix E. During expert clinical review on a subset of 75 questions, only one question was assessed as unanswerable, and 86.7% of the question-answer pairs were evaluated to be clinically relevant. The main dataset limitations were assessed to be the ambiguity in a very small subset of questions, such as four questions relying on inferences of the severity of the underlying conditions as *mild*, *moderate*, or *severe*, without any standardized definitions of these terms. These challenges are reflected in human vs. model performance metrics reported in Table 5.

Table 3: Key statistics for the UCSF-PDGM-VQA dataset

| Size  | Num studies | Avg. words per QA | Avg. series per study | Avg. slices per series |
|-------|-------------|-------------------|-----------------------|------------------------|
| 2,387 | 473         | 188.07            | 23                    | 150.69                 |

### 4.2 Model performance

Table 4: Zero-shot VQA model accuracy (%) on the UCSF-PDGM-VQA dataset. All metrics are averaged over 3 runs. The *MRI* column shows the model accuracy given both the MRI and the question into the model. In the *Single-Slice* setting, the MRI input is the highest tumor-volume slice from the Axial FLAIR scan. The *Multi-Slice* setting includes multiple 2D slices from the MRI, representing the highest tumor volume slices from all axial sequences. In the *3D* setting, the input is the full 3D Nifti volume for Axial FLAIR scan. The *MRI montage* column shows the model accuracy when given both the MRI and the question, where the MRI input is a composite of the highest tumor-volume slices from all axial sequences in the MRI study, as well as containing the tumor and brain segmentation outputs. While single-slice montage refers to a composite of all axial slices, multi-slice montage refers to the use of Axial, Coronal, and Saggital montage as three inputs. The *Blank image* column shows the model accuracy given a blank image and the question. The *Reshuffle* column shows the model’s accuracy when the question choices are shuffled. For all VLMs, this setting includes the same visual input as the *MRI* setting. The *Text-Only* column shows the LLM accuracy when only given the question, without any visual input.

| Model                          | MRI   | MRI montage | Black Image | Reshuffle | Text-Only |
|--------------------------------|-------|-------------|-------------|-----------|-----------|
| Qwen3-8B                       | -     | -           | -           | 47.73     | 52.57     |
| LLaVA-Med-1.5                  | 59.14 | 59.60       | 59.05       | 40.55     | -         |
| MedImageInsight                | 20.77 | 29.69       | 18.68       | 28.01     | -         |
| Med3DVLM-Qwen-2.5-7B - 3D      | 26.91 | -           | 42.42       | 38.55     | -         |
| Lingshu-32B                    | 61.40 | 63.20       | 66.04       | 52.17     | -         |
| MedGemma-1.5-4B - Single Slice | 55.37 | 51.69       | 43.38       | 43.38     | -         |
| MedGemma-1.5-4B - Multi Slice  | 63.57 | 59.08       | -           | 51.16     | -         |
| GPT5-mini - Single Slice       | 34.70 | 38.59       | 32.39       | 19.87     | 18.57     |
| GPT5-mini - Multi Slice        | 23.67 | 27.45       | -           | 22.19     | -         |

Table 4 provides the average zero-shot accuracy of the evaluated models on the UCSF-PDGM-VQA dataset. Similarly, Table 5 contextualizes model performance against clinical performance

Table 5: Model performance on the human evaluation subset, comprising 75 QA pairs, compared to neuro-radiology fellow performance. Retaining only the most promising models based on performance on the complete dataset.

| Setting                      | MRI   | MRI montage |
|------------------------------|-------|-------------|
| Human                        | 87.88 | -           |
| MedGemma-1.5-4B Single slice | 72.73 | 60.61       |
| MedGemma-1.5-4B Multi slice  | 66.67 | 66.67       |
| Lingshu-32B                  | 57.07 | 64.14       |
| Qwen3-8B LLM                 | 53.03 | -           |

on a subset of 75 QA pairs. Evaluations on the UCSF-PDGM-VQA dataset reveal a significant performance gap; among the models tested, the MedGemma-1.5 model, within multiple-slice and single-slice settings, achieved the highest accuracy at 63.57% and 55.37%, respectively. Performance improvement of nearly 8% through multiple slice inputs suggests that the model relies on additional sequences for accurate inference, which also aligns clinically with the expected behavior. MRI montage input harmed the model performance, indicating its inability to process composite images. Even within the highest-performing models, the gap compared to the clinical performance is large (nearly 15%), with the neuro-radiology fellow performance upper bound on the human evaluation subset being nearly 88%. This highlights the limitations of specialist medical VLMs in interpreting multi-sequence, multi-slice brain MRI inputs. Although the Lingshu and LLaVA-med models seem to be performing similarly, ablation settings are concerning and discussed later. The GPT5-mini model struggled to make inferences from multiple images as the input, demonstrating large performance drops compared to single slice settings. Even within single slice or montage settings, the model performance was quite low, which demonstrates the lack of reliable performance for brain MRI inference. The MedImageInsight and the Med3DVLM models, despite being customized for medical data, only performed at random for brain MRI VQA, additionally demonstrating the lack of their inference capability in this domain.

Within the ablation settings, we noticed very interesting findings. The Lingshu model and the LLaVA-Med model, despite their higher performance in the MRI and MRI montage settings, performed similarly when given a black image as input. These results highlight a strong bias toward language priors and the ordering of options in multiple-choice QA settings. Of note is that the Lingshu model includes brain MRI data in its model training data, and the lack of generalizability stems despite that. Furthermore, although the Med3DVLM model performed at random with MRI input, its performance improved significantly when the MRI input was removed or when the option order was shuffled, thus indicating its inability to process brain MRI scans. This is expected since the model was not trained on brain MRI data. MedGemma model performance dropped when provided with black image inputs, indicating its reliance on input MRI data. The GPT5-mini model, however, performed similarly when provided with a black image as input as compared to a single FLAIR MRI slice, highlighting its inability to process that single slice effectively.

Table 6: Example of Questions LLM got correct when provided no image

| Questions  |
|--|
| What are the locations involved by the multifocal hemorrhagic high-grade glial neoplasm?   |
| What are the locations of the two synchronous masses (presumed diffuse glioma)?  |
| What is the anterior location of the tumor’s extension within the temporal lobe?   |
| What is the draining location of the large developmental venous anomaly (DVA) at the superomedial aspect of the right temporal lobe tumor? |
| What is the imaging extent/location of the surrounding edema?  |
| What is the location and extent of the abnormal infiltrative T2 signal?  |
| What is the location of mucosal sinus thickening?  |
| What is the location of the abnormal FLAIR signal?   |

Moreover, Qwen3-8B text-only model, without any image input, surprisingly demonstrated strong performance when provided only with the question and options. At nearly 50% accuracy, the models performed twice as well as random, matching the performance of the best VLM under reshuffled input settings. Table 6 provides a subset of the questions that Qwen3-8B was able to answer correctly

despite its lack of image input. This finding indicates a strong prior in LLMs towards question-answering tasks, as additionally reflected in other VLM ablation experiments, such as the use of blank image input. This suggests that LLMs contribute more strongly towards VLM outputs compared to vision inputs themselves. Interestingly, the text-only inference within the GPT5-mini model did not demonstrate the same pattern, performing poorly even compared to random baselines. However, the model performance even in VLM settings is low, thus suggesting its inability to perform inferences related to brain tumor MRI more generally.

Finally, across most models, we observed large (often 10% or more) performance drops when shuffling the order of options in the question. This suggests a strong bias in the models towards the position of the correct answer. This may be expected given that the questions and their options were generated using an LLM. We further investigated a potential order bias in the options in the generated dataset. We identified that the first option corresponded with the correct answer 84.7% of the time, option 2 — 12.2%, option 3 — 2.7%, and option 4 was correct only in 0.5% of the questions. This highlighted two major vulnerabilities: (a) LLMs, specifically the GPT-4o model, generated the correct option first before adding incorrect options, and (b) vision-language models were able to exploit this vulnerability even in zero-shot inference settings. In the final public version of the dataset, we provide both shuffled and unshuffled options, with the shuffled case as the default for inference, to enable robust benchmarking while also enabling reproducibility.

## 5 Discussion

Popular clinical vision-language models have leveraged and adapted general vision encoders to better capture key regions in medical images, while adjusting their vision-text fusion strategies to improve the model’s understanding of the input data. However, even with these architectural changes, challenges remain with the VLM’s comprehension of domain-specific knowledge and with correctly encoding medical images and fusing them with text tokens. Specifically, current models are limited in their ability to process 3D volumes natively, with most expecting only a limited number of 2D slices as input. This poses a significant constraint for domains such as neuro-oncology, where accurate interpretation relies on a joint inference of multiple 3D imaging sequences at once, which the current models are incapable of processing. This is, in turn, reflected within model performance on real-world benchmarks for brain MRI interpretation. In this study, we developed a new VQA dataset specific to neuro-oncology, pairing multi-sequence brain MRI scans with clinically relevant question-answer pairs to enable benchmarking of VLM performance in realistic clinical settings. Through this dataset, we identified significant gaps in current model capability. Even in closed-ended QA settings, the best models achieved only 64% accuracy, demonstrating a significant gap compared to both clinical needs and the clinical performance upper-bound. This performance is expected to only worsen in open-ended settings. Poor accuracy is driven in part by the lack of models capable of encoding multi-sequence 3D MRI volumes for reliable brain interpretation, and in part by their inability to leverage visual evidence and over-reliance on linguistic patterns.

As also discussed previously by Asadi et al. [2026], current VLMs are susceptible to modality collapse, especially in medical settings. While the previous study identified these limitations in the context of existing clinical vision-language datasets for tasks other than VQA, our study confirmed modality collapse during VQA for interpreting glioma MRIs. Although during clinical evaluations, it was noted that the imaging data was necessary for model inference, most models performed similarly with and without imaging input. Both improved and at-par performance of several models when using a blank image input or a text-only LLM suggests that the VLMs are not reasoning well enough with the MRIs to draw meaningful analysis from the input images, or do not consider the images useful enough when answering the question. Some examples where we witnessed modality collapse included questions related to tumor size, tumor location, and the underlying diagnosis, which are all critically dependent on an individual’s MRI scans. The fact that models can answer these questions without vision inputs is deeply concerning. This underscores the need for model architectures that enforce strict visual grounding and reduced reliance on language priors for grounded, accurate inference over brain MRI scans. Inability to overcome modality collapse, and yet obtaining high performance on tasks that are clinically unanswerable without underlying imaging data, will result in dangerous clinical hallucinations and put patients at a critical safety risk.

## 6 Conclusions

We created a clinically relevant benchmark of 2,387 closed-ended visual question-answer pairs, corresponding to 497 multi-series 3D brain MRI studies, and released it publicly to enable future studies. Through an analysis on this benchmark, we identified: (a) significant performance gaps between existing VLMs and the minimum performance required to enable practical use, thus highlighting a need to improve models for brain MRI VQA, and (b) modality collapse, a key limitation of currently popular medical vision-language models in closed-ended VQA over brain MRIs. Insufficient encoding of volumetric MRI data prevents existing models from effectively leveraging critical information in MRI scans and mapping them to the corresponding text inputs, leading to incorrect VQA inference. This raises a key safety challenge for the potential future deployment of VLMs in clinical settings.

## 7 Limitations and Future Directions

Key limitations of this study are the reliance on imaging data from a single institution, for a single radiologic modality (MRI), for a single disease group (diffuse gliomas), a single anatomy (brain), and a single time point (pre-operative). Thus the results can only be interpreted within these contexts. Furthermore, although we opted for a multiple-choice setting in this study to enable automated evaluation in clinically relevant task setups, the eventual goal is to enable a pathway towards multi-turn conversations within radiologic settings, where users can interact with a vision-language model in an open-ended manner to assist with speedier MRI analysis. To this end, future research will incorporate multi-turn, open-conversational settings, with access to longitudinal scans and patients' clinical history, thus simulating realistic dialogue alongside reasoning-driven responses, as opposed to multiple-choice settings proposed in the current study.

## References

- Kumar Krishna Agrawal, Long Lian, Longchao Liu, Natalia Harguindeguy, Boyi Li, Alexander Bick, Maggie Chung, Trevor Darrell, and Adam Yala. Atlas: Multi-scale attention improves long context image modeling. *arXiv preprint arXiv:2503.12355*, 2025a.
- Kumar Krishna Agrawal, Longchao Liu, Long Lian, Michael Nercessian, Natalia Harguindeguy, Yufu Wu, Peter Mikhael, Gigin Lin, Lecia V. Sequist, Florian Fintelmann, Trevor Darrell, Yutong Bai, Maggie Chung, and Adam Yala. Pillar-0: A new frontier for radiology foundation models. *arXiv preprint arXiv:2511.17803*, 2025b.
- Altaib Al Yassin, Mohammad Salehi Sadaghiani, Suyash Mohan, R Nick Bryan, and Ilya Nasrallah. It is about "time": Academic neuroradiologist time distribution for interpreting brain mris. *Academic Radiology*, 25(12):1521–1525, 2018.
- Mohammad Asadi, Jack W O'Sullivan, Fang Cao, Tahoura Nedae, Kamyar Fardi, Fei-Fei Li, Ehsan Adeli, and Euan Ashley. Mirage the illusion of visual understanding. *arXiv preprint arXiv:2603.21687*, 2026.
- Gorkem Can Ates, Yu Xin, Kuang Gong, and Wei Shao. Dcformer: Efficient 3d vision-language modeling with decomposed convolutions. *arXiv preprint arXiv:2502.05091*, 2025.
- Seongsu Bae, Daeun Kyung, Jaehee Ryu, Eunbyeol Cho, Gyubok Lee, Sunjun Kweon, Jeongwoo Oh, Lei Ji, Eric I-Chao Chang, Tackeun Kim, and Edward Choi. Ehrxqa: a multi-modal question answering dataset for electronic health records with chest x-ray images. In *Proceedings of the 37th International Conference on Neural Information Processing Systems, NIPS '23*, Red Hook, NY, USA, 2023. Curran Associates Inc.
- Fan Bai, Yuxin Du, Tiejun Huang, Max Q-H Meng, and Bo Zhao. M3D: Advancing 3D medical image analysis with multi-modal large language models. *arXiv preprint arXiv:2404.00578*, 2024.
- Shuai Bai, Keqin Chen, Xuejing Liu, Jialin Wang, Wenbin Ge, Sibao Song, Kai Dang, Peng Wang, Shijie Wang, Jun Tang, Humen Zhong, Yuanzhi Zhu, Mingkun Yang, Zhaohai Li, Jianqiang Wan, Pengfei Wang, Wei Ding, Zheren Fu, Yiheng Xu, Jiabo Ye, Xi Zhang, Tianbao Xie, Zesen Cheng, Hang Zhang, Zhibo Yang, Haiyang Xu, and Junyang Lin. Qwen2.5-vl technical report, 2025. URL <https://arxiv.org/abs/2502.13923>.

- Ujjwal Baid, Satyam Ghodasara, Suyash Mohan, Michel Bilello, Evan Calabrese, Errol Colak, Keyvan Farahani, Jayashree Kalpathy-Cramer, Felipe C. Kitamura, Sarthak Pati, Luciano M. Prevedello, Jeffrey D. Rudie, Chiharu Sako, Russell T. Shinohara, Timothy Bergquist, Rong Chai, James Eddy, Julia Elliott, Walter Reade, Thomas Schaffter, Thomas Yu, Jiabin Zheng, Ahmed W. Moawad, Luiz Otavio Coelho, Olivia McDonnell, Elka Miller, Fanny E. Moron, Mark C. Oswood, Robert Y. Shih, Loizos Siakallis, Yulia Bronstein, James R. Mason, Anthony F. Miller, Gagandeep Choudhary, Aanchal Agarwal, Cristina H. Besada, Jamal J. Derakhshan, Mariana C. Diogo, Daniel D. Do-Dai, Luciano Farage, John L. Go, Mohiuddin Hadi, Virginia B. Hill, Michael Iv, David Joyner, Christie Lincoln, Eyal Lotan, Asako Miyakoshi, Mariana Sanchez-Montano, Jaya Nath, Xuan V. Nguyen, Manal Nicolas-Jilwan, Johanna Ortiz Jimenez, Kerem Ozturk, Bojan D. Petrovic, Chintan Shah, Lubdha M. Shah, Manas Sharma, Onur Simsek, Achint K. Singh, Salil Soman, Volodymyr Statsevych, Brent D. Weinberg, Robert J. Young, Ichiro Ikuta, Amit K. Agarwal, Sword C. Cambren, Richard Silbergleit, Alexandru Dusoi, Alida A. Postma, Laurent Letourneau-Guillon, Gloria J. Guzman Perez-Carrillo, Atin Saha, Neetu Soni, Greg Zaharchuk, Vahe M. Zohrabian, Yingming Chen, Milos M. Cekic, Akm Rahman, Juan E. Small, Varun Sethi, Christos Davatzikos, John Mongan, Christopher Hess, Soonmee Cha, Javier Villanueva-Meyer, John B. Freymann, Justin S. Kirby, Benedikt Wiestler, Priscila Crivellaro, Rivka R. Colen, Aikaterini Kotrotsou, Daniel Marcus, Mikhail Milchenko, Arash Nazeri, Hassan Fathallah-Shaykh, Roland Wiest, Andras Jakab, Marc-Andre Weber, Abhishek Mahajan, Bjoern Menze, Adam E. Flanders, and Spyridon Bakas. The rsna-asnr-miccai brats 2021 benchmark on brain tumor segmentation and radiogenomic classification, 2021. URL <https://arxiv.org/abs/2107.02314>.
- Asma Ben Abacha, Mourad Sarrouiti, Dina Demner-Fushman, Sadid A. Hasan, and Henning Müller. Overview of the vqa-med task at imageclef 2021: Visual question answering and generation in the medical domain. In *CLEF 2021 Working Notes*, CEUR Workshop Proceedings, Bucharest, Romania, September 21-24 2021. CEUR-WS.org.
- Louis Blankemeier, Ashwin Kumar, Joseph Paul Cohen, Jiaming Liu, Longchao Liu, Dave Van Veen, Syed Jamal Safdar Gardezi, Hongkun Yu, Magdalini Paschali, Zhihong Chen, Jean-Benoit Delbrouck, Eduardo Reis, Robbie Holland, Cesar Truys, Christian Bluethgen, Yufu Wu, Long Lian, Malte Engmann Kjeldskov Jensen, Sophie Ostmeier, Maya Varma, Jeya Maria Jose Valanarasu, Zhongnan Fang, Zepeng Huo, Zaid Nabulsi, Diego Ardila, Wei-Hung Weng, Edson Amaro Junior, Neera Ahuja, Jason Fries, Nigam H. Shah, Greg Zaharchuk, Marc Willis, Adam Yala, Andrew Johnston, Robert D. Boutin, Andrew Wentland, Curtis P. Langlotz, Jason Hom, Sergios Gatidis, and Akshay S. Chaudhari. Merlin: a computed tomography vision-language foundation model and dataset. *Nature*, 2026. doi: 10.1038/s41586-026-10181-8. URL <https://doi.org/10.1038/s41586-026-10181-8>.
- Benedikt Boecking, Naoto Usuyama, Shruthi Bannur, Daniel C. Castro, Anton Schwaighofer, Stephanie Hyland, Maria Wetscherek, Tristan Naumann, Aditya Nori, Javier Alvarez-Valle, Hoifung Poon, and Ozan Oktay. Making the most of text semantics to improve biomedical vision-language processing. In *Computer Vision – ECCV 2022: 17th European Conference, Tel Aviv, Israel, October 23–27, 2022, Proceedings, Part XXXVI*, page 1–21, Berlin, Heidelberg, 2022. Springer-Verlag. ISBN 978-3-031-20058-8. doi: 10.1007/978-3-031-20059-5\_1. URL [https://doi.org/10.1007/978-3-031-20059-5\\_1](https://doi.org/10.1007/978-3-031-20059-5_1).
- Evan Calabrese, Javier E. Villanueva-Meyer, Jeffrey D. Rudie, Andreas M. Rauschecker, Ujjwal Baid, Spyridon Bakas, Soonmee Cha, John T. Mongan, and Christopher P. Hess. The University of California San Francisco Preoperative Diffuse Glioma MRI (UCSF-PDGM), 2022a. URL <https://www.cancerimagingarchive.net/collection/ucsf-pdgm/>.
- Evan Calabrese, Javier E. Villanueva-Meyer, Jeffrey D. Rudie, Andreas M. Rauschecker, Ujjwal Baid, Spyridon Bakas, Soonmee Cha, John T. Mongan, and Christopher P. Hess. The university of california san francisco preoperative diffuse glioma mri dataset. *Radiology: Artificial Intelligence*, 4(6):e220058, 2022b. doi: 10.1148/ryai.220058. URL <https://doi.org/10.1148/ryai.220058>. PMID: 35146430.
- Wei-Lin Chiang, Zhuohan Li, Zi Lin, Ying Sheng, Zhanghao Wu, Hao Zhang, Lianmin Zheng, Siyuan Zhuang, Yonghao Zhuang, Joseph E. Gonzalez, Ion Stoica, and Eric P. Xing. Vicuna: An open-source chatbot impressing gpt-4 with 90%\* chatgpt quality, March 2023. URL <https://lmsys.org/blog/2023-03-30-vicuna/>.

- Noel C. F. Codella, Ying Jin, Shrey Jain, Yu Gu, Ho Hin Lee, Asma Ben Abacha, Alberto Santamaria-Pang, Will Guyman, Naiteek Sangani, Sheng Zhang, Hoifung Poon, Stephanie Hyland, Shruthi Bannur, Javier Alvarez-Valle, Xue Li, John Garrett, Alan McMillan, Gaurav Rajguru, Madhu Maddi, Nilesh Vijayrania, Rehaan Bhimai, Nick Mecklenburg, Rupal Jain, Daniel Holstein, Naveen Gaur, Vijay Aski, Jenq-Neng Hwang, Thomas Lin, Ivan Tarapov, Matthew Lungren, and Mu Wei. Medimageinsight: An open-source embedding model for general domain medical imaging, 2024. URL <https://arxiv.org/abs/2410.06542>.
- Nikhil J. Dhinagar, Chirag Jagad, Pavithra Senthilkumar, Sophia I. Thomopoulos, Mahir H. Khan, Sook-Lei Liew, the ENIGMA-Stroke Recovery Working Group, Nerisa Banaj, Michael R. Boric, Lara A. Boyd, Amy Brodtmann, Jessica M. Cassidy, Adriana B. Conforto, Steven C. Cramer, Adrienne N. Dula, Fatemeh Geranmayeh, Chris M. Gregory, Brenton Hordacre, Abhishek Jaywant, Steven A. Kautz, Kristan A. Leech, Martin Lotze, Maria Mataró, Fabrizio Piras, Emily R. Rosario, Nerses Sanossian, Heidi M. Schambra, Nicolas Schweighofer, Na Jin Seo, Surjo R. Soekadar, Gregory T. Thielman, Carolee Winstein, George F. Wittenberg, Kristin A. Wong, and Paul M. Thompson. Calm-vlm: Calibration and selective prediction in vision–language models for reliable brain mri classification. *bioRxiv*, 2026. doi: 10.64898/2026.04.10.717865. URL <https://www.biorxiv.org/content/early/2026/04/14/2026.04.10.717865>.
- Mingyu Ding, Bin Xiao, Noel Codella, Ping Luo, Jingdong Wang, and Lu Yuan. Davit: Dual attention vision transformers. In *European conference on computer vision*, pages 74–92. Springer, 2022.
- Sedigheh Eslami, Christoph Meinel, and Gerard De Melo. PubMedClip: How much does clip benefit visual question answering in the medical domain? In *Findings of the Association for Computational Linguistics: EACL 2023*, pages 1181–1193, 2023.
- Ibrahim Ethem Hamamci, Sezgin Er, Chenyu Wang, Furkan Almas, Ayse Gulnihan Simsek, Seval Nil Esirgun, Irem Dogan, Omer Faruk Durugol, Benjamin Hou, Suprosanna Shit, Weicheng Dai, Murong Xu, Hadrien Reynaud, Muhammed Furkan Dasdelen, Bastian Wittmann, Tamaz Amiranashvili, Enis Simsar, Mehmet Simsar, Emine Bensus Erdemir, Abdullah Alanbay, Anjany Sekuboyina, Berkan Lafci, Ahmet Kaplan, Zhiyong Lu, Malgorzata Polacin, Bernhard Kainz, Christian Bluethgen, Kayhan Batmanghelich, Mehmet Kemal Ozdemir, and Bjoern Menze. Generalist foundation models from a multimodal dataset for 3d computed tomography. *Nature Biomedical Engineering*, February 2026. ISSN 2157-846X. doi: 10.1038/s41551-025-01599-y. URL <http://dx.doi.org/10.1038/s41551-025-01599-y>.
- Ali Hatamizadeh, Vishwesh Nath, Yucheng Tang, Dong Yang, Holger R Roth, and Daguang Xu. Swin UNETR: Swin transformers for semantic segmentation of brain tumors in MRI images. In *International MICCAI brainlesion workshop*, pages 272–284. Springer, 2021.
- Xuehai He, Yichen Zhang, Luntian Mou, Eric Xing, and Pengtao Xie. PathVQA: 30000+ questions for medical visual question answering. *arXiv preprint arXiv:2003.10286*, 2020.
- Xinyue Hu, Lin Gu, Qiyuan An, Mengliang Zhang, liangchen liu, Kazuma Kobayashi, Tatsuya Harada, Ronald Summers, and Yingying Zhu. Medical-Diff-VQA: A Large-Scale Medical Dataset for Difference Visual Question Answering on Chest X-Ray Images. *PhysioNet*, February 2025. doi: 10.13026/e6dd-cn74. URL <https://doi.org/10.13026/e6dd-cn74>. Version 1.0.1.
- Yefan Huang, Xiaoli Wang, Feiyan Liu, and Guofeng Huang. Ovqa: A clinically generated visual question answering dataset. In *Proceedings of the 45th International ACM SIGIR Conference on Research and Development in Information Retrieval*, pages 2924–2938, 2022.
- Olga Kovaleva, Chaitanya P. Shivade, Satyananda Kashyap, Karina Kanjaria, Adam Coy, Deddeh Balah, Yufan Guo, Joy T. Wu, Alexandros Karargyris, David James Beymer, Anna Rumshisky, and Vandana V. Mukherjee. Visual dialog for radiology: Data curation and firststeps. In *ViGIL@NeurIPS*, 2019. URL <https://api.semanticscholar.org/CorpusID:208615597>.
- E. A. Krupinski, K. S. Berbaum, R. T. Caldwell, K. M. Scharztz, and J. Kim. Long radiology workdays reduce detection and accommodation accuracy. *Journal of the American College of Radiology*, 7(9):698–704, 2010. doi: 10.1016/j.jacr.2010.03.004.

- Jason J Lau, Soumya Gayen, Asma Ben Abacha, and Dina Demner-Fushman. A dataset of clinically generated visual questions and answers about radiology images. *Scientific data*, 5(1):180251, 2018.
- Chunyu Li, Cliff Wong, Sheng Zhang, Naoto Usuyama, Haotian Liu, Jianwei Yang, Tristan Naumann, Hoifung Poon, and Jianfeng Gao. Llava-med: Training a large language-and-vision assistant for biomedicine in one day. *Advances in Neural Information Processing Systems*, 36: 28541–28564, 2023.
- Yikuan Li, Ramsey M. Wehbe, Faraz S. Ahmad, Hanyin Wang, and Yuan Luo. Clinical-Longformer and clinical-BigBird: Transformers for long clinical sequences, 2022. URL <https://arxiv.org/abs/2201.11838>.
- Bo Liu, Li-Ming Zhan, Li Xu, Lin Ma, Yan Yang, and Xiao-Ming Wu. Slake: A semantically-labeled knowledge-enhanced dataset for medical visual question answering. In *2021 IEEE 18th international symposium on biomedical imaging (ISBI)*, pages 1650–1654. IEEE, 2021.
- Yiwei Lyu, Samir Harake, Asadur Chowdury, Soumyanil Banerjee, Rachel Gologorsky, Shixuan Liu, Anna-Katharina Meissner, Akshay Rao, Chenhui Zhao, Akhil Kondepudi, Cheng Jiang, Xinhai Hou, Rushikesh S. Joshi, Volker Neuschmelting, Ashok Srinivasan, Dawn O Kleindorfer, Brian D. Athey, Vikas Gulani, Aditya Pandey, Honglak Lee, and Todd C. Hollon. Learning neuroimaging models from health system-scale data. *Nature biomedical engineering*, 2026. URL <https://api.semanticscholar.org/CorpusID:285343811>.
- Deepali Mishra, Chaklam Silpasuwanchai, Ashutosh Modi, Madhumita Sushil, and Sorayouth Chumnanvej. Barriers in integrating medical visual question answering into radiology workflows: A scoping review and clinicians’ insights. *arXiv preprint arXiv:2507.08036*, 2025.
- Michael Moor, Qian Huang, Shirley Wu, Michihiro Yasunaga, Yash Dalmia, Jure Leskovec, Cyril Zakka, Eduardo Pontes Reis, and Pranav Rajpurkar. Med-Flamingo: a multimodal medical few-shot learner. In *Machine learning for health (ML4H)*, pages 353–367. PMLR, 2023.
- Vishwesh Nath, Wenqi Li, Dong Yang, Andriy Myronenko, Mingxin Zheng, Yao Lu, Zhijian Liu, Hongxu Yin, Yucheng Tang, Pengfei Guo, Can Zhao, Ziyue Xu, Yufan He, Greg Heinrich, Yee Man Law, Benjamin Simon, Stephanie Harmon, Stephen Aylward, Marc Edgar, Michael Zephyr, Song Han, Pavlo Molchanov, Baris Turkbey, Holger Roth, and Daguang Xu. Vila-m3: Enhancing vision-language models with medical expert knowledge, 2025. URL <https://arxiv.org/abs/2411.12915>.
- OpenAI. Introducing GPT-5.2 — openai.com. <https://openai.com/index/introducing-gpt-5-2/>, 2025. [Accessed 02-05-2026].
- OpenAI, :, Aaron Hurst, Adam Lerer, Adam P. Goucher, Adam Perelman, Aditya Ramesh, Aidan Clark, AJ Ostrow, Akila Welihinda, Alan Hayes, Alec Radford, Aleksander Mądry, Alex Baker-Whitcomb, Alex Beutel, Alex Borzunov, Alex Carney, Alex Chow, Alex Kirillov, Alex Nichol, Alex Paino, Alex Renzin, Alex Tachard Passos, Alexander Kirillov, Alexi Christakis, Alexis Conneau, Ali Kamali, Allan Jabri, Allison Moyer, Allison Tam, Amadou Crookes, Amin Tootoochian, Amin Tootoonchian, Ananya Kumar, Andrea Vallone, Andrej Karpathy, Andrew Braunstein, Andrew Cann, Andrew Codispoti, Andrew Galu, Andrew Kondrich, Andrew Tulloch, Andrey Mishchenko, Angela Baek, Angela Jiang, Antoine Pelisse, Antonia Woodford, Anuj Gosalia, Arka Dhar, Ashley Pantuliano, Avi Nayak, Avital Oliver, Barret Zoph, Behrooz Ghorbani, Ben Leimberger, Ben Rossen, Ben Sokolowsky, Ben Wang, Benjamin Zweig, Beth Hoover, Blake Samic, Bob McGrew, Bobby Spero, Bogo Giertler, Bowen Cheng, Brad Lightcap, Brandon Walkin, Brendan Quinn, Brian Guarraci, Brian Hsu, Bright Kellogg, Brydon Eastman, Camillo Lugaresi, Carroll Wainwright, Cary Bassin, Cary Hudson, Casey Chu, Chad Nelson, Chak Li, Chan Jun Shern, Channing Conger, Charlotte Barette, Chelsea Voss, Chen Ding, Cheng Lu, Chong Zhang, Chris Beaumont, Chris Hallacy, Chris Koch, Christian Gibson, Christina Kim, Christine Choi, Christine McLeavey, Christopher Hesse, Claudia Fischer, Clemens Winter, Coley Czarnecki, Colin Jarvis, Colin Wei, Constantin Koumouzelis, Dane Sherburn, Daniel Kappler, Daniel Levin, Daniel Levy, David Carr, David Farhi, David Mely, David Robinson, David Sasaki, Denny Jin, Dev Valladares, Dimitris Tsipras, Doug Li, Duc Phong Nguyen, Duncan Findlay, Edele Oiwoh, Edmund Wong, Ehsan Asdar, Elizabeth Proehl, Elizabeth Yang, Eric Antonow, Eric

Kramer, Eric Peterson, Eric Sigler, Eric Wallace, Eugene Brevdo, Evan Mays, Farzad Khorasani, Felipe Petroski Such, Filippo Raso, Francis Zhang, Fred von Lohmann, Freddie Sulit, Gabriel Goh, Gene Oden, Geoff Salmon, Giulio Starace, Greg Brockman, Hadi Salman, Haiming Bao, Haitang Hu, Hannah Wong, Haoyu Wang, Heather Schmidt, Heather Whitney, Heewoo Jun, Hendrik Kirchner, Henrique Ponde de Oliveira Pinto, Hongyu Ren, Huiwen Chang, Hyung Won Chung, Ian Kivlichan, Ian O’Connell, Ian O’Connell, Ian Osband, Ian Silber, Ian Sohl, Ibrahim Okuyucu, Ikai Lan, Ilya Kostrikov, Ilya Sutskever, Ingmar Kanitscheider, Ishaan Gulrajani, Jacob Coxon, Jacob Menick, Jakub Pachocki, James Aung, James Betker, James Crooks, James Lennon, Jamie Kiros, Jan Leike, Jane Park, Jason Kwon, Jason Phang, Jason Teplitz, Jason Wei, Jason Wolfe, Jay Chen, Jeff Harris, Jenia Varavva, Jessica Gan Lee, Jessica Shieh, Ji Lin, Jiahui Yu, Jiayi Weng, Jie Tang, Jieqi Yu, Joanne Jang, Joaquin Quinonero Candela, Joe Beutler, Joe Landers, Joel Parish, Johannes Heidecke, John Schulman, Jonathan Lachman, Jonathan McKay, Jonathan Uesato, Jonathan Ward, Jong Wook Kim, Joost Huizinga, Jordan Sitkin, Jos Kraaijeveld, Josh Gross, Josh Kaplan, Josh Snyder, Joshua Achiam, Joy Jiao, Joyce Lee, Juntang Zhuang, Justyn Harriman, Kai Fricke, Kai Hayashi, Karan Singhal, Katy Shi, Kavin Karthik, Kayla Wood, Kendra Rimbach, Kenny Hsu, Kenny Nguyen, Keren Gu-Lemberg, Kevin Button, Kevin Liu, Kiel Howe, Krithika Muthukumar, Kyle Luther, Lama Ahmad, Larry Kai, Lauren Itow, Lauren Workman, Leher Pathak, Leo Chen, Li Jing, Lia Guy, Liam Fedus, Liang Zhou, Lien Mamitsuka, Lilian Weng, Lindsay McCallum, Lindsey Held, Long Ouyang, Louis Feuvrier, Lu Zhang, Lukas Kondraciuk, Lukasz Kaiser, Luke Hewitt, Luke Metz, Lyric Doshi, Mada Aflak, Maddie Simens, Madelaine Boyd, Madeleine Thompson, Marat Dukhan, Mark Chen, Mark Gray, Mark Hudnall, Marvin Zhang, Marwan Aljube, Mateusz Litwin, Matthew Zeng, Max Johnson, Maya Shetty, Mayank Gupta, Meghan Shah, Mehmet Yatbaz, Meng Jia Yang, Mengchao Zhong, Mia Glaese, Mianna Chen, Michael Janner, Michael Lampe, Michael Petrov, Michael Wu, Michele Wang, Michelle Fradin, Michelle Pokrass, Miguel Castro, Miguel Oom Temudo de Castro, Mikhail Pavlov, Miles Brundage, Miles Wang, Minal Khan, Mira Murati, Mo Bavarian, Molly Lin, Murat Yesildal, Nacho Soto, Natalia Gimelshein, Natalie Cone, Natalie Staudacher, Natalie Summers, Natan LaFontaine, Neil Chowdhury, Nick Ryder, Nick Stathas, Nick Turley, Nik Tezak, Niko Felix, Nithanth Kudige, Nitish Keskar, Noah Deutsch, Noel Bundick, Nora Puckett, Ofir Nachum, Ola Okelola, Oleg Boiko, Oleg Murk, Oliver Jaffe, Olivia Watkins, Olivier Godement, Owen Campbell-Moore, Patrick Chao, Paul McMillan, Pavel Belov, Peng Su, Peter Bak, Peter Bakkum, Peter Deng, Peter Dolan, Peter Hoeschele, Peter Welinder, Phil Tillet, Philip Pronin, Philippe Tillet, Prafulla Dhariwal, Qiming Yuan, Rachel Dias, Rachel Lim, Rahul Arora, Rajan Troll, Randall Lin, Rapha Gontijo Lopes, Raul Puri, Reah Miyara, Reimar Leike, Renaud Gaubert, Reza Zamani, Ricky Wang, Rob Donnelly, Rob Honsby, Rocky Smith, Rohan Sahai, Rohit Ramchandani, Romain Huet, Rory Carmichael, Rowan Zellers, Roy Chen, Ruby Chen, Ruslan Nigmatullin, Ryan Cheu, Saachi Jain, Sam Altman, Sam Schoenholz, Sam Toizer, Samuel Miserendino, Sandhini Agarwal, Sara Culver, Scott Ethersmith, Scott Gray, Sean Grove, Sean Metzger, Shamez Hermani, Shantanu Jain, Shengjia Zhao, Sherwin Wu, Shino Jomoto, Shirong Wu, Shuaiqi, Xia, Sonia Phene, Spencer Papay, Srinivas Narayanan, Steve Coffey, Steve Lee, Stewart Hall, Suchir Balaji, Tal Broda, Tal Stramer, Tao Xu, Tarun Gogineni, Taya Christianson, Ted Sanders, Tejal Patwardhan, Thomas Cunningham, Thomas Degry, Thomas Dimson, Thomas Raoux, Thomas Shadwell, Tianhao Zheng, Todd Underwood, Todor Markov, Toki Sherbakov, Tom Rubin, Tom Stasi, Tomer Kaftan, Tristan Heywood, Troy Peterson, Tyce Walters, Tyna Eloundou, Valerie Qi, Veit Moeller, Vinnie Monaco, Vishal Kuo, Vlad Fomenko, Wayne Chang, Weiyi Zheng, Wenda Zhou, Wesam Manassra, Will Sheu, Wojciech Zaremba, Yash Patil, Yilei Qian, Yongjik Kim, Youlong Cheng, Yu Zhang, Yuchen He, Yuchen Zhang, Yujia Jin, Yunxing Dai, and Yury Malkov. Gpt-4o system card, 2024. URL <https://arxiv.org/abs/2410.21276>.

Mackenzie Price, Christine Ballard, Julia Benedetti, Corey Neff, Gino Cioffi, Kristin A Waite, Carol Kruchko, Jill S Barnholtz-Sloan, and Quinn T Ostrom. CBTRUS statistical report: primary brain and other central nervous system tumors diagnosed in the united states in 2017–2021. *Neuro-oncology*, 26(Suppl 6):vi1, 2024.

Qwen, :, An Yang, Baosong Yang, Beichen Zhang, Binyuan Hui, Bo Zheng, Bowen Yu, Chengyuan Li, Dayiheng Liu, Fei Huang, Haoran Wei, Huan Lin, Jian Yang, Jianhong Tu, Jianwei Zhang, Jianxin Yang, Jiaxi Yang, Jingren Zhou, Junyang Lin, Kai Dang, Keming Lu, Keqin Bao, Kexin Yang, Le Yu, Mei Li, Mingfeng Xue, Pei Zhang, Qin Zhu, Rui Men, Runji Lin, Tianhao Li, Tianyi Tang, Tingyu Xia, Xingzhang Ren, Xuancheng Ren, Yang Fan, Yang Su, Yichang Zhang, Yu Wan,

- Yuqiong Liu, Zeyu Cui, Zhenru Zhang, and Zihan Qiu. Qwen2.5 technical report, 2025. URL <https://arxiv.org/abs/2412.15115>.
- Alec Radford, Jeff Wu, Rewon Child, David Luan, Dario Amodei, and Ilya Sutskever. Language models are unsupervised multitask learners. 2019. URL <https://api.semanticscholar.org/CorpusID:160025533>.
- Alec Radford, Jong Wook Kim, Chris Hallacy, Aditya Ramesh, Gabriel Goh, Sandhini Agarwal, Girish Sastry, Amanda Askell, Pamela Mishkin, Jack Clark, Gretchen Krueger, and Ilya Sutskever. Learning transferable visual models from natural language supervision. In *International Conference on Machine Learning*, 2021. URL <https://api.semanticscholar.org/CorpusID:231591445>.
- Andrew Sellergren, Sahar Kazemzadeh, Tiam Jaroensri, Atilla Kiraly, Madeleine Traverse, Timo Kohlberger, Shawn Xu, Fayaz Jamil, Cían Hughes, Charles Lau, Justin Chen, Fereshteh Mahvar, Liron Yatziv, Tiffany Chen, Bram Sterling, Stefanie Anna Baby, Susanna Maria Baby, Jeremy Lai, Samuel Schmidgall, Lu Yang, Kejia Chen, Per Bjornsson, Shashir Reddy, Ryan Brush, Kenneth Philbrick, Mercy Asiedu, Ines Mezerreg, Howard Hu, Howard Yang, Richa Tiwari, Sunny Jansen, Preeti Singh, Yun Liu, Shekoofeh Azizi, Aishwarya Kamath, Johan Ferret, Shreya Pathak, Nino Vieillard, Ramona Merhej, Sarah Perrin, Tatiana Matejovicova, Alexandre Ramé, Morgane Riviere, Louis Rouillard, Thomas Mesnard, Geoffrey Cideron, Jean bastien Grill, Sabela Ramos, Edouard Yvinec, Michelle Casbon, Elena Buchatskaya, Jean-Baptiste Alayrac, Dmitry Lepikhin, Vlad Feinberg, Sebastian Borgeaud, Alek Andreev, Cassidy Hardin, Robert Dadashi, Léonard Hussenot, Armand Joulin, Olivier Bachem, Yossi Matias, Katherine Chou, Avinatan Hassidim, Kavi Goel, Clement Farabet, Joelle Barral, Tris Warkentin, Jonathon Shlens, David Fleet, Victor Cotruta, Omar Sanseviero, Gus Martins, Phoebe Kirk, Anand Rao, Shravya Shetty, David F. Steiner, Can Kirmizibayrak, Rory Pilgrim, Daniel Golden, and Lin Yang. MedGemma technical report. *arXiv preprint arXiv:2507.05201*, 2025.
- Aaditya Singh, Adam Fry, Adam Perelman, Adam Tart, Adi Ganesh, Ahmed El-Kishky, Aidan McLaughlin, Aiden Low, AJ Ostrow, Akhila Ananthram, Akshay Nathan, Alan Luo, Alec Helyar, Aleksander Madry, Aleksandr Efremov, Aleksandra Spyra, Alex Baker-Whitcomb, Alex Beutel, Alex Karpenko, Alex Makelov, Alex Neitz, Alex Wei, Alexandra Barr, Alexandre Kirchmeyer, Alexey Ivanov, Alexi Christakis, Alistair Gillespie, Allison Tam, Ally Bennett, Alvin Wan, Alyssa Huang, Amy McDonald Sandjideh, Amy Yang, Ananya Kumar, Andre Saraiva, Andrea Vallone, Andrei Gheorghie, Andres Garcia Garcia, Andrew Braunstein, Andrew Liu, Andrew Schmidt, Andrew Mereskin, Andrew Mishchenko, Andy Applebaum, Andy Rogerson, Ann Rajan, Annie Wei, Anoop Kotha, Anubha Srivastava, Anushree Agrawal, Arun Vijayvergiya, Ashley Tyra, Ashvin Nair, Avi Nayak, Ben Eggers, Bessie Ji, Beth Hoover, Bill Chen, Blair Chen, Boaz Barak, Borys Minaiev, Botao Hao, Bowen Baker, Brad Lightcap, Brandon McKinzie, Brandon Wang, Brendan Quinn, Brian Fioca, Brian Hsu, Brian Yang, Brian Yu, Brian Zhang, Brittany Brenner, Callie Riggin Zetino, Cameron Raymond, Camillo Lugaresi, Carolina Paz, Cary Hudson, Cedric Whitney, Chak Li, Charles Chen, Charlotte Cole, Chelsea Voss, Chen Ding, Chen Shen, Chengdu Huang, Chris Colby, Chris Hallacy, Chris Koch, Chris Lu, Christina Kaplan, Christina Kim, CJ Minott-Henriques, Cliff Frey, Cody Yu, Coley Czarnecki, Colin Reid, Colin Wei, Cory Decareaux, Cristina Scheau, Cyril Zhang, Cyrus Forbes, Da Tang, Dakota Goldberg, Dan Roberts, Dana Palmie, Daniel Kappler, Daniel Levine, Daniel Wright, Dave Leo, David Lin, David Robinson, Declan Grabb, Derek Chen, Derek Lim, Derek Salama, Dibya Bhattacherjee, Dimitris Tsipras, Dinghua Li, Dingli Yu, DJ Strouse, Drew Williams, Dylan Hunn, Ed Bayes, Edwin Arbus, Ekin Akyurek, Elaine Ya Le, Elana Widmann, Eli Yani, Elizabeth Proehl, Enis Sert, Enoch Cheung, Eri Schwartz, Eric Han, Eric Jiang, Eric Mitchell, Eric Sigler, Eric Wallace, Erik Ritter, Erin Kavanaugh, Evan Mays, Evgenii Nikishin, Fangyuan Li, Felipe Petroski Such, Filipe de Avila Belbute Peres, Filippo Raso, Florent Bekerman, Foivos Tsimpourlas, Fotis Chantzis, Francis Song, Francis Zhang, Gaby Raila, Garrett McGrath, Gary Briggs, Gary Yang, Giambattista Parascandolo, Gildas Chabot, Grace Kim, Grace Zhao, Gregory Valiant, Guillaume Leclerc, Hadi Salman, Hanson Wang, Hao Sheng, Haoming Jiang, Haoyu Wang, Haozhun Jin, Harshit Sikchi, Heather Schmidt, Henry Aspegren, Honglin Chen, Huida Qiu, Hunter Lightman, Ian Covert, Ian Kivlichan, Ian Silber, Ian Sohl, Ibrahim Hammoud, Ignasi Clavera, Ikai Lan, Ilge Akkaya, Ilya Kostrikov, Irina Kofman, Isak Etinger, Ishaan Singal, Jackie Hehir, Jacob Huh, Jacqueline Pan, Jake Wilczynski, Jakob Pachocki, James Lee, James Quinn, Jamie Kiros, Janvi Kalra, Jasmyn Samaroo, Jason Wang, Jason Wolfe,

Jay Chen, Jay Wang, Jean Harb, Jeffrey Han, Jeffrey Wang, Jennifer Zhao, Jeremy Chen, Jerene Yang, Jerry Tworek, Jesse Chand, Jessica Landon, Jessica Liang, Ji Lin, Jiancheng Liu, Jianfeng Wang, Jie Tang, Jihan Yin, Joanne Jang, Joel Morris, Joey Flynn, Johannes Ferstad, Johannes Heidecke, John Fishbein, John Hallman, Jonah Grant, Jonathan Chien, Jonathan Gordon, Jongsoo Park, Jordan Liss, Jos Kraaijeveld, Joseph Guay, Joseph Mo, Josh Lawson, Josh McGrath, Joshua Vendrow, Joy Jiao, Julian Lee, Julie Steele, Julie Wang, Junhua Mao, Kai Chen, Kai Hayashi, Kai Xiao, Kamyar Salahi, Kan Wu, Karan Sekhri, Karan Sharma, Karan Singhal, Karen Li, Kenny Nguyen, Keren Gu-Lemberg, Kevin King, Kevin Liu, Kevin Stone, Kevin Yu, Kristen Ying, Kristian Georgiev, Kristie Lim, Kushal Tirumala, Kyle Miller, Lama Ahmad, Larry Lv, Laura Clare, Laurance Fauconnet, Lauren Itow, Lauren Yang, Laurentia Romaniuk, Leah Anise, Lee Byron, Leher Pathak, Leon Maksin, Leyan Lo, Leyton Ho, Li Jing, Liang Wu, Liang Xiong, Lien Mamitsuka, Lin Yang, Lindsay McCallum, Lindsey Held, Liz Bourgeois, Logan Engstrom, Lorenz Kuhn, Louis Feuvrier, Lu Zhang, Lucas Switzer, Lukas Kondraciuk, Lukasz Kaiser, Manas Joglekar, Mandeep Singh, Mandip Shah, Manuka Stratta, Marcus Williams, Mark Chen, Mark Sun, Marselus Cayton, Martin Li, Marvin Zhang, Marwan Aljube, Matt Nichols, Matthew Haines, Max Schwarzer, Mayank Gupta, Meghan Shah, Melody Y. Guan, Melody Huang, Meng Dong, Mengqing Wang, Mia Glaese, Micah Carroll, Michael Lampe, Michael Malek, Michael Sharman, Michael Zhang, Michele Wang, Michelle Pokrass, Mihai Florian, Mikhail Pavlov, Miles Wang, Ming Chen, Mingxuan Wang, Minnia Feng, Mo Bavarian, Molly Lin, Moose Abdool, Mostafa Rohaninejad, Nacho Soto, Natalie Staudacher, Natan LaFontaine, Nathan Marwell, Nelson Liu, Nick Preston, Nick Turley, Nicklas Ansmann, Nicole Blades, Nikil Pancha, Nikita Mikheylin, Niko Felix, Nikunj Handa, Nishant Rai, Nitish Keskar, Noam Brown, Ofir Nachum, Oleg Boiko, Oleg Murk, Olivia Watkins, Oona Gleeson, Pamela Mishkin, Patryk Lesiewicz, Paul Baltescu, Pavel Belov, Peter Zhokhov, Philip Pronin, Phillip Guo, Phoebe Thacker, Qi Liu, Qiming Yuan, Qinghua Liu, Rachel Dias, Rachel Puckett, Rahul Arora, Ravi Teja Mullapudi, Raz Gaon, Reah Miyara, Rennie Song, Rishabh Aggarwal, RJ Marsan, Robel Yemiru, Robert Xiong, Rohan Kshirsagar, Rohan Nuttall, Roman Tsiupa, Ronen Eldan, Rose Wang, Roshan James, Roy Ziv, Rui Shu, Ruslan Nigmatullin, Saachi Jain, Saam Talaie, Sam Altman, Sam Arnesen, Sam Toizer, Sam Toyer, Samuel Miserendino, Sandhini Agarwal, Sarah Yoo, Savannah Heon, Scott Ethersmith, Sean Grove, Sean Taylor, Sebastian Bubeck, Sever Banesiu, Shaokyi Amdo, Shengjia Zhao, Sherwin Wu, Shibani Santurkar, Shiyu Zhao, Shraman Ray Chaudhuri, Shreyas Krishnaswamy, Shuaiqi, Xia, Shuyang Cheng, Shyamal Anadkat, Simón Posada Fishman, Simon Tobin, Siyuan Fu, Somay Jain, Song Mei, Sonya Egoian, Spencer Kim, Spug Golden, SQ Mah, Steph Lin, Stephen Imm, Steve Sharpe, Steve Yadlowsky, Sulman Choudhry, Sungwon Eum, Suvansh Sanjeev, Tabarak Khan, Tal Stramer, Tao Wang, Tao Xin, Tarun Gogineni, Taya Christianson, Ted Sanders, Tejal Patwardhan, Thomas Degry, Thomas Shadwell, Tianfu Fu, Tianshi Gao, Timur Garipov, Tina Sriskandarajah, Toki Sherbakov, Tomek Korbak, Tomer Kaftan, Tomo Hiratsuka, Tongzhou Wang, Tony Song, Tony Zhao, Troy Peterson, Val Kharitonov, Victoria Chernova, Vineet Kosaraju, Vishal Kuo, Vitvich Pong, Vivek Verma, Vlad Petrov, Wanning Jiang, Weixing Zhang, Wenda Zhou, Wenlei Xie, Wenting Zhan, Wes McCabe, Will DePue, Will Ellsworth, Wulfie Bain, Wyatt Thompson, Xiangning Chen, Xiangyu Qi, Xin Xiang, Xinwei Shi, Yann Dubois, Yaodong Yu, Yara Khakbaz, Yifan Wu, Yilei Qian, Yin Tat Lee, Yinbo Chen, Yizhen Zhang, Yizhong Xiong, Yonglong Tian, Young Cha, Yu Bai, Yu Yang, Yuan Yuan, Yuanzhi Li, Yufeng Zhang, Yuguang Yang, Yujia Jin, Yun Jiang, Yunyun Wang, Yushi Wang, Yutian Liu, Zach Stubenvoll, Zehao Dou, Zheng Wu, and Zhigang Wang. OpenAI gpt-5 system card, 2026. URL <https://arxiv.org/abs/2601.03267>.

Gemma Team, Aishwarya Kamath, Johan Ferret, Shreya Pathak, Nino Vieillard, Ramona Merhej, Sarah Perrin, Tatiana Matejovicova, Alexandre Ramé, Morgane Rivière, Louis Rouillard, Thomas Mesnard, Geoffrey Cideron, Jean-Bastien Grill, Sabela Ramos, Edouard Yvinec, Michelle Casbon, Etienne Pot, Ivo Penchev, Gaël Liu, Francesco Visin, Kathleen Kenealy, Lucas Beyer, Xiaohai Zhai, Anton Tsitsulin, Robert Busa-Fekete, Alex Feng, Naveen Sachdeva, Benjamin Coleman, Yi Gao, Basil Mustafa, Iain Barr, Emilio Parisotto, David Tian, Matan Eyal, Colin Cherry, Jan-Thorsten Peter, Danila Sinopalnikov, Surya Bhupatiraju, Rishabh Aggarwal, Mehran Kazemi, Dan Malkin, Ravin Kumar, David Vilar, Idan Brusilovsky, Jiaming Luo, Andreas Steiner, Abe Friesen, Abhanshu Sharma, Abheesht Sharma, Adi Mayrav Gilady, Adrian Goedeckemeyer, Alaa Saade, Alex Feng, Alexander Kolesnikov, Alexei Bendebury, Alvin Abdagic, Amit Vadi, András György, André Susano Pinto, Anil Das, Ankur Bapna, Antoine Miech, Antoine Yang, Antonia Paterson, Ashish Shenoy, Ayan Chakrabarti, Bilal Piot, Bo Wu, Bobak Shahriari, Bryce Pettrini, Charlie Chen, Charline Le Lan, Christopher A. Choquette-Choo, CJ Carey, Cormac Brick, Daniel

- Deutsch, Danielle Eisenbud, Dee Cattle, Derek Cheng, Dimitris Paparas, Divyashree Shivakumar Sreepathihalli, Doug Reid, Dustin Tran, Dustin Zelle, Eric Noland, Erwin Huizenga, Eugene Kharitonov, Frederick Liu, Gagik Amirkhanyan, Glenn Cameron, Hadi Hashemi, Hanna Klimczak-Plucińska, Harman Singh, Harsh Mehta, Harshal Tushar Lehri, Hussein Hazimeh, Ian Ballantyne, Idan Szpektor, Ivan Nardini, Jean Pouget-Abadie, Jetha Chan, Joe Stanton, John Wieting, Jonathan Lai, Jordi Orbay, Joseph Fernandez, Josh Newlan, Ju yeong Ji, Jyotinder Singh, Kat Black, Kathy Yu, Kevin Hui, Kiran Vodrahalli, Klaus Greff, Linhai Qiu, Marcella Valentine, Marina Coelho, Marvin Ritter, Matt Hoffman, Matthew Watson, Mayank Chaturvedi, Michael Moynihan, Min Ma, Nabila Babar, Natasha Noy, Nathan Byrd, Nick Roy, Nikola Momchev, Nilay Chauhan, Noveen Sachdeva, Oskar Bunyan, Pankil Botarda, Paul Caron, Paul Kishan Rubenstein, Phil Culliton, Philipp Schmid, Pier Giuseppe Sessa, Pingmei Xu, Piotr Stanczyk, Pouya Tafti, Rakesh Shivanna, Renjie Wu, Renke Pan, Reza Rokni, Rob Willoughby, Rohith Vallu, Ryan Mullins, Sammy Jerome, Sara Smoot, Sertan Girgin, Shariq Iqbal, Shashir Reddy, Shruti Sheth, Siim Pöder, Sijal Bhatnagar, Sindhu Raghuram Panyam, Sivan Eiger, Susan Zhang, Tianqi Liu, Trevor Yacovone, Tyler Liechty, Uday Kalra, Utku Evcı, Vedant Misra, Vincent Roseberry, Vlad Feinberg, Vlad Kolesnikov, Woo Hyun Han, Woosuk Kwon, Xi Chen, Yinlam Chow, Yuvein Zhu, Zichuan Wei, Zoltan Egyed, Victor Cotruta, Minh Giang, Phoebe Kirk, Anand Rao, Kat Black, Nabila Babar, Jessica Lo, Erica Moreira, Luiz Gustavo Martins, Omar Sanseviero, Lucas Gonzalez, Zach Gleicher, Tris Warkentin, Vahab Mirrokni, Evan Senter, Eli Collins, Joelle Barral, Zoubin Ghahramani, Raia Hadsell, Yossi Matias, D. Sculley, Slav Petrov, Noah Fiedel, Noam Shazeer, Oriol Vinyals, Jeff Dean, Demis Hassabis, Koray Kavukcuoglu, Clement Farabet, Elena Buchatskaya, Jean-Baptiste Alayrac, Rohan Anil, Dmitry, Lepikhin, Sebastian Borgeaud, Olivier Bachem, Armand Joulin, Alek Andreev, Cassidy Hardin, Robert Dadashi, and Léonard Hussenot. Gemma 3 technical report, 2025a. URL <https://arxiv.org/abs/2503.19786>.
- LASA Team, Weiwen Xu, Hou Pong Chan, Long Li, Mahani Aljunied, Ruifeng Yuan, Jianyu Wang, Chenghao Xiao, Guizhen Chen, Chaoqun Liu, Zhaodonghui Li, Yu Sun, Junao Shen, Chaojun Wang, Jie Tan, Deli Zhao, Tingyang Xu, Hao Zhang, and Yu Rong. Lingshu: A generalist foundation model for unified multimodal medical understanding and reasoning, 2025b. URL <https://arxiv.org/abs/2506.07044>.
- Hugo Touvron, Thibaut Lavril, Gautier Izacard, Xavier Martinet, Marie-Anne Lachaux, Timothée Lacroix, Baptiste Rozière, Naman Goyal, Eric Hambro, Faisal Azhar, Aurelien Rodriguez, Armand Joulin, Edouard Grave, and Guillaume Lample. Llama: Open and efficient foundation language models, 2023. URL <https://arxiv.org/abs/2302.13971>.
- Javier E Villanueva-Meyer, Marc C Mabray, and Soonmee Cha. Current clinical brain tumor imaging. *Neurosurgery*, 81(3):397–415, 2017.
- Guangyu Wang, Xiaohong Liu, Zhen Ying, Guoxing Yang, Zhiwei Chen, Zhiwen Liu, Min Zhang, Hongmei Yan, Yuxing Lu, Yuanxu Gao, Kanmin Xue, Xiaoying Li, and Ying Chen. Optimized glycemic control of type 2 diabetes with reinforcement learning: a proof-of-concept trial. *Nature Medicine*, 29:2633 – 2642, 2023. URL <https://api.semanticscholar.org/CorpusID:261884154>.
- Yu Xin, Gorkem Can Ates, Kuang Gong, and Wei Shao. Med3dVLM: An efficient vision-language model for 3d medical image analysis. *IEEE Journal of Biomedical and Health Informatics*, 2025.
- An Yang, Anfeng Li, Baosong Yang, Beichen Zhang, Binyuan Hui, Bo Zheng, Bowen Yu, Chang Gao, Chengen Huang, Chenxu Lv, Chujie Zheng, Dayiheng Liu, Fan Zhou, Fei Huang, Feng Hu, Hao Ge, Haoran Wei, Huan Lin, Jialong Tang, Jian Yang, Jianhong Tu, Jianwei Zhang, Jianxin Yang, Jiayi Yang, Jing Zhou, Jingren Zhou, Junyang Lin, Kai Dang, Keqin Bao, Kexin Yang, Le Yu, Lianghao Deng, Mei Li, Mingfeng Xue, Mingze Li, Pei Zhang, Peng Wang, Qin Zhu, Rui Men, Ruize Gao, Shixuan Liu, Shuang Luo, Tianhao Li, Tianyi Tang, Wenbiao Yin, Xingzhang Ren, Xinyu Wang, Xinyu Zhang, Xuancheng Ren, Yang Fan, Yang Su, Yichang Zhang, Yinger Zhang, Yu Wan, Yuqiong Liu, Zekun Wang, Zeyu Cui, Zhenru Zhang, Zhipeng Zhou, and Zihan Qiu. Qwen3 technical report, 2025. URL <https://arxiv.org/abs/2505.09388>.
- Jianwei Yang, Chunyuan Li, Pengchuan Zhang, Bin Xiao, Ce Liu, Lu Yuan, and Jianfeng Gao. Unified contrastive learning in image-text-label space. In *Proceedings of the IEEE/CVF conference on computer vision and pattern recognition*, pages 19163–19173, 2022.

- Lu Yuan, Dongdong Chen, Yi-Ling Chen, Noel Codella, Xiyang Dai, Jianfeng Gao, Houdong Hu, Xuedong Huang, Boxin Li, Chunyuan Li, Ce Liu, Mengchen Liu, Zicheng Liu, Yumao Lu, Yu Shi, Lijuan Wang, Jianfeng Wang, Bin Xiao, Zhen Xiao, Jianwei Yang, Michael Zeng, Luowei Zhou, and Pengchuan Zhang. Florence: A new foundation model for computer vision, 2021. URL <https://arxiv.org/abs/2111.11432>.
- Ke Zhang, Yan Yang, Jun Yu, Hanliang Jiang, Jianping Fan, Qingming Huang, and Weidong Han. Multi-task paired masking with alignment modeling for medical vision-language pre-training. *IEEE Transactions on Multimedia*, 26:4706–4721, 2023a.
- Sheng Zhang, Yanbo Xu, Naoto Usuyama, Hanwen Xu, Jaspreet Bagga, Robert Tinn, Sam Preston, Rajesh Rao, Mu Wei, Naveen Valluri, Cliff Wong, Andrea Tupini, Yu Wang, Matt Mazzola, Swadheen Shukla, Lars Liden, Jianfeng Gao, Angela Crabtree, Brian Piening, Carlo Bifulco, Matthew P. Lungren, Tristan Naumann, Sheng Wang, and Hoifung Poon. A multimodal biomedical foundation model trained from fifteen million image–text pairs. *NEJM AI*, 2(1):AIoa2400640, 2025. doi: 10.1056/AIoa2400640. URL <https://ai.nejm.org/doi/full/10.1056/AIoa2400640>.
- Xiaoman Zhang, Chaoyi Wu, Ziheng Zhao, Weixiong Lin, Ya Zhang, Yanfeng Wang, and Weidi Xie. PMC-VQA: Visual instruction tuning for medical visual question answering. *arXiv preprint arXiv:2305.10415*, 2023b.
- Lianmin Zheng, Wei-Lin Chiang, Ying Sheng, Siyuan Zhuang, Zhanghao Wu, Yonghao Zhuang, Zi Lin, Zhuohan Li, Dacheng Li, Eric P. Xing, Hao Zhang, Joseph E. Gonzalez, and Ion Stoica. Judging llm-as-a-judge with mt-bench and chatbot arena. In *Proceedings of the 37th International Conference on Neural Information Processing Systems, NIPS '23*, Red Hook, NY, USA, 2023. Curran Associates Inc.

## A QA Pair Generation Settings and Prompt

For the generation phase, we adjusted the GPT-4o LLM to have a temperature of 0.15 to increase the strictness of this process and prevent the LLM from deviating from the guidelines in the prompt. We accessed this model via the Versa API to ensure data security.

The generation prompt is as follows:

```
You will be given the radiology report of a patient. Your job is to
create question-answer pairs based on the information given in the
'IMPRESSION' and 'FINDING' sections of the report.

Each question MUST have 4 options, 1 correct option and 3 incorrect
options, and these options MUST be in the same string as the
question. You MUST create 20 question-answer pairs

EXAMPLE QUESTION FORMAT:
Where is the location of the tumor?

1) Upper Left Region  2) Upper Right Region  3) Lower Left Region  4)
  Lower Right Region

EXAMPLE ANSWER FORMAT:
Upper Right Region

CREATE QUESTION-ANSWER PAIRS BASED ON THE INFORMATION BELOW:
- Please answer the following list of questions and provide the
  reasoning for each answer.
- Please format the response so that the reasoning is clearly
  separated from the answer.
- Place the reasoning section before the answer.
- Please quote direct full sentences of evidence from the report in
  the reasoning section to help justify the answer.
- Each question will provide the multiple options of the answer, pick
  one of them and follow the instructions on how to answer.
- An answer of "no" means that the report specifically confirms the
  answer to the question is no and there is clear evidence to
  confirm this.
- A reasoning of "inconclusive" means "insufficient conclusive
  evidence" or that there might be some evidence to indicate some
  answer, but there isn't enough to confidently conclude an answer.
- An answer of "not discussed" means "not discussed in the report" or
  that the question topic was not mentioned in the report at all.
  Keep the original numbering for the list of questions.
- DO NOT include any questions that are not related to the "IMPRESSION
  " and "FINDINGS" sections.
- DO NOT include any follow-up questions or questions that REQUIRE
  knowledge outside of the report
- DO NOT include any questions that ask about 'residual' portions of
  the tumor or questions about a previous MRI
- DO NOT use the phrase 'in the report' in the questions. The
  questions should be answerable with only the MRI.
- ALL ANSWERS should be in the text and should never be "None of the
  Above"

RADIOLOGY REPORT:
(radiology report)
```

## B QA Pair Generation Output Structure

The generation phase JSON output structure is as follows:

```
{  
  'question' : str,  
  'answer' : str,  
  'reasoning' : str  
}
```

## C QA Pair Validation Prompt

For the validation phase, we adjusted the GPT-5.2 LLM to have a temperature of 0.15 to increase the strictness of this process and prevent the LLM from deviating from the guidelines in the prompt. We accessed this model through the Versa API for data security.

The validation prompt is as follows:

```
Given a radiology report for a brain MRI, please go through each of
the question-answer pairs and determine if the pairs can be
answered given the criteria below.

Please answer the following list of questions and provide the
reasoning for each answer.
Please format the response so that the reasoning is clearly separated
from the answer.
Place the reasoning section before the answer.
Please quote direct full sentences of evidence from the report in the
reasoning section to help justify the answer.
Each question will provide the multiple options of the answer, pick
one of them and follow the instructions on how to answer.
Keep the original numbering for the list of questions.
If the question-answer pairs MEETS any of the criteria below, then tag
them with the "NO" string.
If the question-answer pairs does NOT MEET any of the criteria below,
then tag them with the "YES" string.
Also, be sure to explain why you chose the tag in the 'tag reasoning'
response.

CRITERIA:
- ANY question-answer pairs that require the patient's clinical
  history, previous brain MRIs, or any other information outside of
  the report to answer (Questions about "midline shift" are ok and
  should NOT be tagged 'NO')
- ANY question-answer pairs with the reasoning of "Inconclusive" and
  nothing else
- ANY question-answer pairs with the answer of "Not discussed" and
  nothing else
- ANY questions that explicitly asks to compare the MRI with a
  previous MRI or ask about a previous MRI. (Some keywords:
  postsurgical changes, postsurgical, retrospect, progression,
  recurrent, stable, tumor growth, tumor shrinkage, metastasis)
- ANY questions that REQUIRE knowledge outside of the report to answer
  it.
- ANY questions that ask about 'residual' portions of the tumor.
- ANY question-answer pairs with the answer of "None of the above".
- ANY question-answer pairs where it asks what technique is being used
  in the report in an explicit or implicit manner. (Some keywords:
  multivoxel spectroscopy, FLAIR, T1, T2)
- ANY questions that are not related to the brain
- ANY questions that are not about aspects found in the brain MRI

You also have the ability to change questions if they do not meet the
QUESTION CHANGING CRITERIA below.
Your job is to look over the input question-answer pair and make the
changes to the questions and answers based on the information
given in the 'IMPRESSION' and 'FINDING' sections of the report.
ONLY MAKE CHANGES if the question-answer pair meets the criteria below
that show which questions need to be changed and how they should
be changed, otherwise keep everything the same.
Do NOT add 'based on the report' in any of the questions.

Your outputted question MUST contain a new question or the original
question.
```

Your output choices MUST include FOUR potential choices. ONE should be the answer based on the report, the others should be changed to more easily differentiate the incorrect choices from the correct one, or be the same as the original choices.

Your outputted answer MUST be ONE of the potential choices and must be based on the radiology report.

QUESTION CHANGING CRITERIA:

- Any questions asking about the size MUST specify what dimensions it is looking for. You MUST add the dimension format used to answer the question

(EX: DIMENSION: (x, y, z) for 5 x 5 x 5 cm. DIMENSION: (x, y) for 5 x 5 cm)

Be sure to space out the potential choices so only one choice is correct within a margin of error (For cm measurements, you MUST have a 1 cm difference between choices. For midline shifts and bigger structures, you MUST have a 5mm difference between choices. For smaller structures, like pituitary gland, you MUST have a 3mm difference between choices.)

- Any questions that are asking about a specific aspect (e.g, lesion, mass, tumor, anything dependent on anatomy) of the MRI MUST be sure to change the question so we know the exact location of where the characteristic is. You MUST be as descriptive as possible when describing the location.

If the location of the specific aspect is unknown, then you MUST include the aspect's laterality.

QUESTION-ANSWER PAIRS:

(QA pairs from the generation phase)

## D QA Pair Validation Output Structure

The validation phase JSON output structure is as follows:

```
{
  'question' : str,
  'answer' : str,
  'reasoning' : str,
  'tag' : str,
  'tag_reasoning' : str
}
```

## E Sample QA Pairs

Table 7: Sample question-answer pairs in the curated UCSF-PDGM-VQA dataset.

| Question  | Answer  |
|---|---|
| What is the location of the cystic lesion? 1) Left frontal lobe 2) Right retrolenticular internal capsule/thalamus 3) Left parietal lobe 4) Right occipital lobe  | Right retrolenticular internal capsule/thalamus |
| What is the observed mass effect on the right lateral ventricle? 1) Compression 2) Expansion 3) No effect 4) Displacement   | Compression                                     |
| What is the measured midline shift (right-to-left) due to mass effect? 1) 9 mm right to left 2) 4 mm right to left 3) 14 mm right to left 4) 7 mm left to right   | 9 mm right to left                              |
| What is the size of the lesion in the left frontal middle gyrus? DIMENSION: (AP x transverse x CC) 1) 3.1 x 2.9 x 3.8 cm 2) 2.1 x 1.9 x 2.8 cm 3) 4.1 x 3.9 x 4.8 cm 4) 1.1 x 0.9 x 1.8 cm  | 3.1 x 2.9 x 3.8 cm                              |
| What is the observed vascularity of the mass centered in the posterior right temporal lobe? 1) Significant hypervascularity 2) Minimal vascularity 3) No vascularity 4) Moderate vascularity                                      | Significant hypervascularity                    |
| Which structure is specifically noted to have surrounding T2 FLAIR hyperintensity extension? 1) Right optic tract 2) Left optic tract 3) Right cerebellar hemisphere 4) Left cerebellar hemisphere                                | Right optic tract                               |
| What is the size of the heterogeneously enhancing lesion centered in the right insula and temporal stem? DIMENSION: (AP, transverse) 1) 4.5 x 3.1 cm 2) 5.5 x 4.1 cm 3) 3.5 x 2.1 cm 4) 6.5 x 5.1 cm                              | 4.5 x 3.1 cm                                    |
| What is the degree of midline shift observed? 1) 2 mm 2) 6 mm 3) 11 mm 4) 16 mm   | 6 mm  |
| What is the size of the mass centered within the left frontotemporal lobes (including the left hippocampus) with involvement of the left insula? DIMENSION: (x, y) 1) 4 x 4 cm 2) 5 x 5 cm 3) 6 x 6 cm 4) 7 x 7 cm                | 6 x 6 cm  |
| What type of enhancement does the large mass centered in the left frontotemporal lobes with involvement of the left insula demonstrate? 1) Thin rim enhancement 2) Thick rim enhancement 3) No enhancement 4) Uniform enhancement | Thick rim enhancement                           |
| What is the observed left-to-right midline shift associated with the left frontotemporal-insular mass? 1) 0.5 cm 2) 1.0 cm 3) 1.5 cm 4) 2.0 cm  | 1.5 cm  |

## F Model Evaluation hyperparameters and set up

All experiments were conducted on an internal high-performance computing cluster equipped with 6 NVIDIA H100 and L40S GPUs and a slurm-based scheduler. The zero-shot inference pipeline for the 2,387 QA pairs across all model configurations (Single-slice, Multi-slice, and Montage) took approximately 818 total GPU hours. Pre-processing of the MRI volumes, including brain tumor segmentation using the Swin-UNETR model, required an additional 48 hours on the same internal cluster. All model hyperparameters are reported in Table 8.

Table 8: Model configurations and inference settings for medical VQA evaluation.

| <b>Model</b>    | <b>Key Inference Settings</b>   |
|-----------------|---|
| MedGemma-1.5-4B | Greedy decoding (do_sample=False), max_new_tokens: 512, bf16/fp16, Structured Output (Pydantic) |
| GPT5-mini       | max_completion_tokens: 4096, Structured Output (Pydantic), "gpt-5-mini-2025-08-07"              |
| Lingshu-32B     | bf16, max_new_tokens: 512, SDPA attention implementation, Structured Output (Pydantic),         |
| LLaVA-Med-1.5   | temperature=.2, do_sample=True  |
| MedImageInsight | CLIP-style zero-shot similarity (no text generation)  |
| Med3DVLM        | Greedy decoding (do_sample=False), max_new_tokens: 512, temperature=0                           |
| Qwen3-8B        | Greedy decoding (do_sample=False),  |